IN SITU STABLE ISOTOPIC EVIDENCE FOR PROTRACTED AND COMPLEX CARBONATE CEMENTATION IN A PETROLEUM RESERVOIR, NORTH COLES LEVEE, SAN JOAQUIN BASIN, CALIFORNIA, U.S.A

MOSTAFA FAYEK,[1]* T. MARK HARRISON,[1] MARTY GROVE,[1] KEVIN D. McKEEGAN,[1] CHRIS D. COATH,[1] AND JAMES R. BOLES[2]
[1] *Department of Earth and Space Sciences and Institute of Geophysical and Planetary Physics, University of California, Los Angeles, California 90095–1567, U.S.A.*
[2] *Department of Geological Sciences, University of California, Santa Barbara, Santa Barbara, California 93106, U.S.A.*
e-mail: mfayek@utk.edu

ABSTRACT: **Knowledge of the evolution of carbonate cementation in hydrocarbon reservoirs is key to understanding the history of fluid flow during petroleum accumulation. The Stevens sands is a sequence of marine shales and deep-sea fan sands that was deposited within the Miocene Monterey Formation in the south-central part of the San Joaquin basin, California, during the upper Miocene (10–6 Ma). Rapid, high-precision *in situ* oxygen and carbon isotopic analyses of carbonate phases using the ion microprobe operated in multi-collection mode, in conjunction with electron microprobe analyses, indicate that carbonate cement zones within the Stevens sands at North Coles Levee (NCL) have had a complex and protracted fluid history. Three main generations of carbonate cement were identified.**

The relative timing of carbonate cement precipitation within the Stevens sands at NCL was estimated using the thermal and burial history of the San Joaquin basin, *in situ* oxygen isotope data, and cementation temperatures derived from equilibrium oxygen isotope fractionation factors for calcite–water and dolomite–water. Precipitation of these cement zones began soon after sediment deposition (~ 7 Ma) and is ongoing. Early dolomite was precipitated at a temperature of ~ 10°C, near the sediment–water interface, and soon after sediment deposition. Calcite cements, which are the most abundant variety, precipitated semicontinuously between 4 Ma and 5 Ma, at temperatures between 50°C and 65°C, and depths of 800 m to 1300 m. Fe-dolomite, which is paragenetically late, appears to have precipitated at temperatures near 100°C in response to pore-pressure reduction, which accompanied exploitation of the gas cap within the last 35 years. Carbon in these cements was likely derived from several sources including marine, maturing hydrocarbons, and a zone of methanogenesis.

INTRODUCTION

Carbonate cements are an important feature of hydrocarbon reservoirs throughout the world (Heald and Larese 1973; Hayes 1979; Boles 1987; Sharp et al. 1988; Boles 1998). These cements restrict fluid flow, thereby enhancing hydrocarbon accumulation (Boles and Ramseyer 1987). Recent studies of sandstone-hosted hydrocarbon reservoirs suggest that cement zones within a single reservoir often have a complex chemistry (Boles 1998) because of changes in the composition of the cementing fluid during diagenetic processes such as compaction, pressure solution, and dissolution (Houseknecht 1987; Pate 1989; Wood and Boles 1991; Taylor and Soule 1993; Robinson et al. 1993; Feldman et al. 1993; Mahon et al. 1998b). However, heterogeneities in deposition and the dynamics of diagenesis can be difficult to assess accurately (Craft and Hawkins 1991). Textural, isotopic, and trace-element data from carbonate cements can potentially provide insight into the scale of pore-water migration, estimates of the temperature at the time of cement formation, and permit characterization of the initial pore-fluid composition. In addition, carbonate cements in clastic-rich basins can contain isotopic and chemical information regarding the source of the dissolved carbon in the evolving pore waters.

The San Joaquin sandstone basin, California, has a young depositional age (< 15 Ma) and a relatively simple subsidence history (Boles 1987; Fischer and Surdam 1988; Hayes and Boles 1992; Taylor and Soule 1993; Mahon et al. 1998a; Boles 1998). In addition, several decades of exploration and development of hydrocarbon resources have produced large quantities of subsurface data. Therefore, the timing of cementation and the composition of multiple fluid events associated with diagenesis potentially can be constrained to a greater degree than for many other basins.

Previous studies (Boles and Ramseyer 1987; Schultz et al. 1989; Wood and Boles 1991; Mahon et al. 1998b) have shown that carbonate cements within the Stevens sandstone at the North Coles Levee (NCL), San Joaquin basin, have a complex mineralogy and experienced a protracted fluid history. Carbonate cement zones often consist of dolomite, calcite, and Fe-dolomite, and chemical and isotopic zonation generally occurs on the scale of micrometers (5–100 μm; Mahon et al. 1998b). Thus, a detailed and accurate fluid history of these carbonate cements is facilitated by *in situ* oxygen and carbon isotopic analysis. This information can be used to shed light on how the cement zones formed and, potentially, the timing of hydrocarbon accumulation.

In this study, we utilize the ion microprobe to perform extensive *in situ* carbon and oxygen isotopic analyses of calcite and dolomite cements associated with the NCL oil field to assess its fluid history. In conjunction with the thermal history previously developed (Mahon et al. 1998a), these results are used to constrain the timing of carbonate cementation, revealing an episodic fluid history that may be typical of sandstone reservoirs.

GEOLOGICAL CONSIDERATIONS

San Joaquin Basin

The San Joaquin basin of California (Fig. 1) began as a forearc basin resulting from Mesozoic subduction and concomitant formation of the Sierra Nevada batholith (Dickinson 1974). The formation of the modern San Joaquin basin largely coincided with the development of the San Andreas transform fault system over the past 8 My (Graham and Williams 1985; Bent 1988). More than 80% of basin fill is of Miocene age or younger (Graham 1987).

The basin consists of nonmarine to marginal marine sands on the flanks, which grade into deep marine shales towards the center (Callaway 1971). The sediments on the east side of the San Joaquin basin rest on the Sierra Nevada batholith, whereas the western flank rests on oceanic crust or the adjoining subduction complex. As a result of transpressional activity associated with the San Andreas fault system, the basin was significantly uplifted and eroded during the Neogene (Boles 1998). The Stevens sandstone, a sequence of marine shales and deep-sea fan sands, was deposited as part of the Miocene Monterey Formation in the south-central part of the basin during the upper Mohnian (10–6 Ma; Callaway 1990). The sands were largely derived from adjacent denuded Cretaceous batholiths (Reid 1990). Anoxic conditions in the deep marine setting were ideal for the preservation of organic-rich rocks (Graham 1987).

Two distinct stages of Cenozoic subsidence can be recognized in the San Joaquin basin. Early subsidence began during the Late Eocene (51 Ma), lasting until the Late Miocene (~ 8 Ma), and was characterized by slow subsidence and little structural deformation (see burial reconstruction in

* Present Address: Department of Geological Sciences, University of Tennessee/Oak Ridge National Laboratory, Knoxville, Tennessee 37996-1410, U.S.A.

JOURNAL OF SEDIMENTARY RESEARCH, VOL. 71, NO. 3, MAY, 2001, P. 444–458
 1073-130X/01/071-444/$03.00

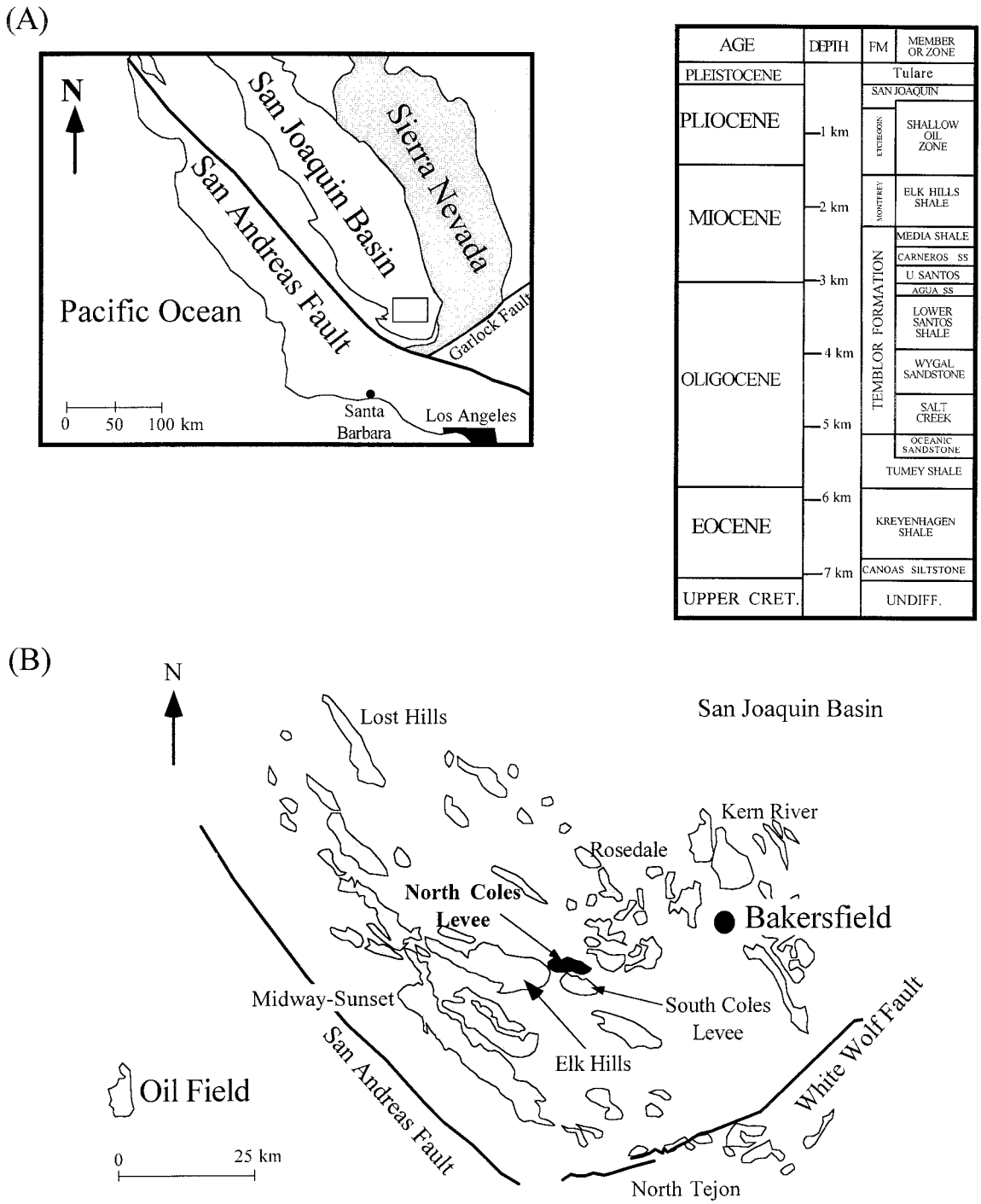

FIG. 1.—**A)** Location map of the San Joaquin basin. The box represents the area of study shown in detail in B. The stratigraphy of the San Joaquin basin in the vicinity of the North Coles Levee is also shown on the right (modified from Reid 1990). **B)** A plan view showing the location of several oil fields that occur within the Stevens sands (projected to the surface) including the North Coles Levee.

Wood and Boles 1991). The second stage of subsidence began ~ 7–8 Ma and continues to the present. This stage of deformation is characterized by the formation of anticlinal structures that presently form the main hydrocarbon traps at North Coles Levee. Sediment accumulation was rapid, ranging from ~ 50 m/Ma to ~ 300 m/Ma during Stevens deposition (upper Mohnian, ~ 10–6 Ma; Lagoie 1987) up to a maximum rate of ~ 600 m/My between 5 My and 6 My, shortly after Stevens deposition. Following this maximum rate, the rate of deposition has decreased to the present (Wood and Boles 1991).

North Coles Levee Oil Field

The North Coles Levee oil field is located on the crest of the Bakersfield arch (Fig. 1). The reservoir, 6.4 km long and 2.8 km wide, is an east–west

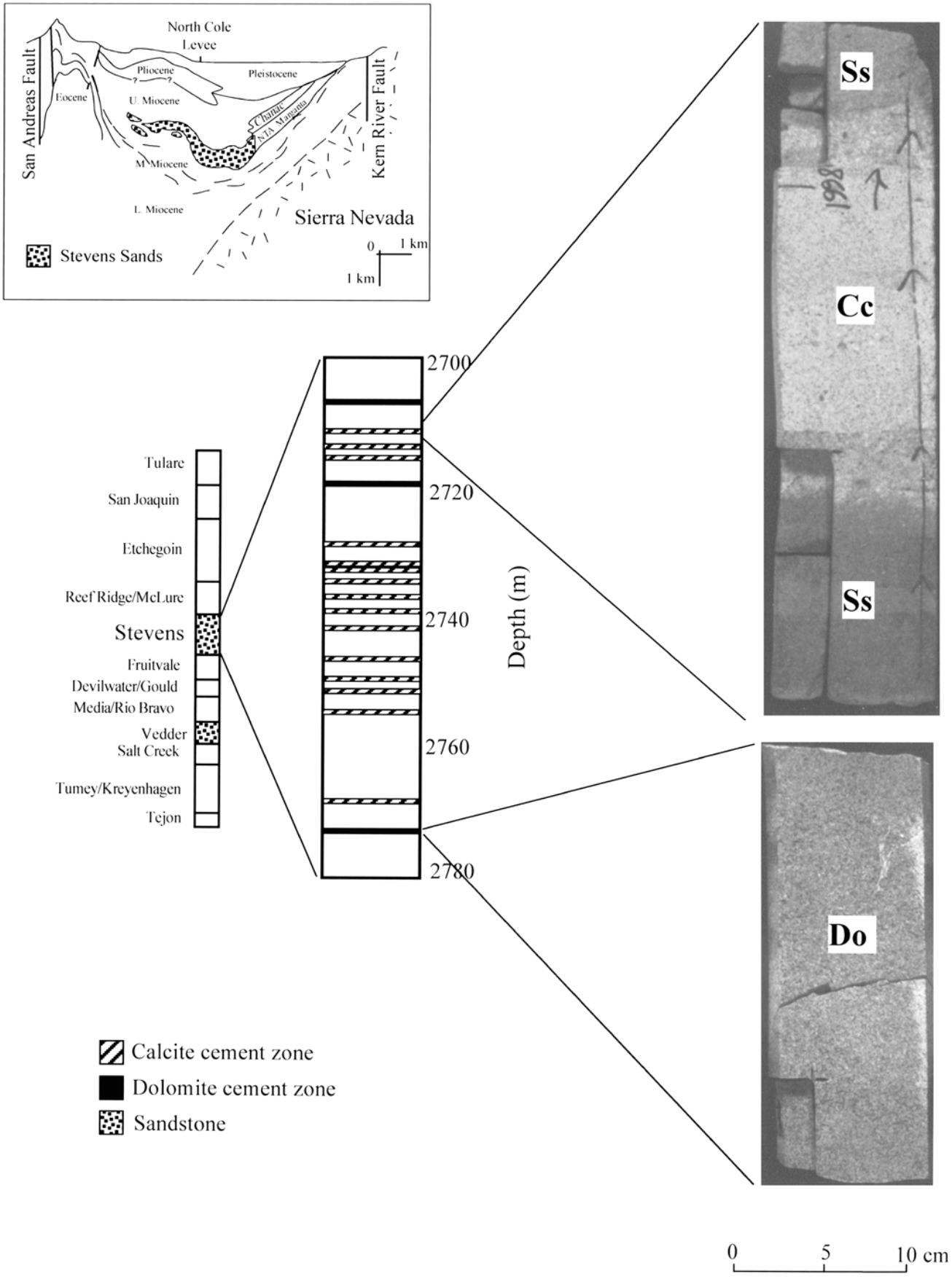
North Cole
Levee
San Andreas Fault
Kern River Fault
Pliocene
Pleistocene
Eocene
U. Miocene
Channel
Antelope
M. Miocene
L. Miocene
Sierra Nevada
Stevens Sands
0 1 km
1 km
Tulare
San Joaquin
Etchegoin
Reef Ridge/McLure
Stevens
Fruitvale
Devilwater/Gould
Media/Rio Bravo
Vedder
Salt Creek
Tumey/Kreyenhagen
Tejon
2700
2720
2740
2760
2780
Depth (m)
Ss
Cc
Ss
Do
Calcite cement zone
Dolomite cement zone
Sandstone
0 5 10 cm

TABLE 1.—*Chemical composition and conventional stable isotopic analyses of standards*

Sample No.	Mineral	CaO (wt%)	FeO (wt%)	MgO (wt%)	MnO (wt%)	CO_2 (wt%)	N	Conventional $\delta^{18}O_{PDB}$ (‰)	Conventional $\delta^{13}C_{PDB}$ (‰)	N	Ion Microprobe $\delta^{18}O_{PDB}$ (‰)
Optical Calcite	Calcite	56.04	0.01	0.00	0.00	43.90	5	−14.4 ± 0.1	−11.1 ± 0.1	21	−14.4 ± 0.6
MM	Calcite	59.00	0.06	0.60	0.07	40.28	5	−2.0 ± 0.1	2.1 ± 0.1	18	−2.1 ± 0.3
MD	Dolomite	32.98	0.12	23.38	0.00	43.52	4	−8.7 ± 0.1	0.98 ± 0.1	13	—
MS1319 UCLA	Fe-dolomite	29.62	6.34	17.46	0.55	46.62	4	−20.3 ± 0.1	−4.4 ± 0.1	10	—
Synthetic Ankerite	Ankerite	24.47	34.69	0.00	0.00	40.74	3	−14.9 ± 0.2	−3.6 ± 0.2	6	

N represents the number of stable isotopic analyses; errors are $1\sigma_{mean}$.

trending anticline that plunges to the east. The main reservoir (Fig. 2; Stevens sandstone) consists of 152 m of amalgamated medium- to fine-grained biotite-rich arenite with 1:1 quartz/feldspar and plagioclase/K-feldspar ratios and less than 25% igneous and metamorphic fragments (Wood and Boles 1991; Boles 1998).

Production is largely from sandstones at a depth of 2500–2865 m with an average porosity of 15% and an average permeability of 10^{-14} m^2 (100 md; Wood and Boles 1991). However, the sandstones contain several thin, discontinuous shale partings, which are less permeable ($\sim 10^{-15}$ m^2; 10 md). Low permeabilities are attributed to poor sorting and abundant clay minerals (Wood and Boles 1991). Permeability barriers that obstruct vertical fluid flow also exist in the form of carbonate cements, which are the focus of this study.

Data collected from wells that have penetrated depths > 5181 m, far below the production interval, have bottom-hole temperatures > 140°C (Wood and Boles 1991). The geothermal gradient in this region, calculated from these bottom-hole temperatures, is between 30 and 40°C/km. Thus, all of the shales below the Stevens Formation in the vicinity of NCL are 100°C or hotter and have either passed through or are presently within the oil window ($\sim$ 60°C to 150°C; Wood and Boles 1991). Two shale units, the Tumey and Kreyenhagen (Fig. 1), have relatively high concentrations of total organic carbon (TOC) and therefore are viable sources for hydrocarbons. However, these units should have generated hydrocarbons during or shortly after Stevens deposition, and thus generation of hydrocarbons from these source rocks preceded development of Stevens calcite cement traps (Wood and Boles 1991).

The main diagenetic alteration at NCL consists of thin, 0.025–1 m layers of calcite- and dolomite-cemented sands and silts (Fig. 2) and partial leaching of detrital plagioclase, forming calcite and kaolinite as byproducts (Boles and Ramseyer 1987; Boles 1998). Biotite shows increasing deformation with burial depth. In addition, the basin has abundant hydrocarbon accumulations that have resulted from organic diagenesis. The oils are found throughout the stratigraphic section, indicating cross-formational flow from deeper levels in the basin (Boles 1998). The pore-waters involved in diagenesis within the central basin were original marine waters and possibly those derived from dehydration reactions (smectite–illite). Presently much of the basin pore-water has salinity similar to seawater, but at deeper levels pore-water composition has been modified by reaction with plagioclase and organic acids (Carothers and Kharaka 1978; MacGowen and Surdam 1988; Fisher and Boles 1990; Feldman et al. 1993).

ANALYTICAL TECHNIQUES

Samples from the calcite- and dolomite-cemented zones from the North Coles Levee (well 488–29; Fig. 2) were selected for the present study. These samples represent the dominant cement zones within the Stevens sands responsible for restricting vertical fluid flow and thereby enhancing hydrocarbon accumulation. Polished thin sections of samples collected from drill core were prepared to determine the mineral paragenesis. Thin sections were examined by transmitted-light microscopy and back-scattered electron imaging (BSE). Chemical compositions of carbonates (Tables 1, 2) were determined by wavelength dispersive spectroscopy (WDS) using a fully automated CAMECA 50 X-ray microanalyzer operated at 15 keV, a beam diameter of 10 μm, and counting times of 40 s per element. Detection limits and precision for the elements (Ca, Fe, Mg, and Mn) were on the order 0.1 wt %. The program PAP was used to reduce data for the various elements. Carbon and oxygen contents of carbonates were calculated by stoichiometry and by difference, respectively.

Polished thin sections of isotopically characterized calcite, dolomite, and Fe-dolomite standards were also prepared. The standards were examined for chemical homogeneity by transmitted light microscopy, BSE, and quantitative electron microprobe analysis, and isotopic homogeneity at the micrometer scale, by measuring their raw (see below) $^{18}O/^{16}O$ and $^{13}C/^{12}C$ ratios by ion probe. A diamond micro-drill (drill tip size 100 μm) was used to sample regions (400 μm in diameter) of the selected carbonate standards. The powders were pulverized using a mortar and pestle, and a smear mount was then prepared. Sample purity was further verified by X-ray diffraction.

Conventional Stable Isotope Analyses of Standards

The multiple fractions obtained by micro-drilling of optical calcite (MS1212G), MM calcite, MD dolomite (from T.K. Kyser), and Fe-dolomite (MS1319), used as internal lab ion microprobe standards, were reacted with 100% H_3PO_4. $\delta^{13}C$ and $\delta^{18}O$ values were determined on CO_2 liberated from carbonates at 25°C for calcite and 50°C for dolomite and Fe-dolomite. These measurements were performed at Queen's University, Canada, using a Finnigan MAT 252 gas source mass spectrometer. All oxygen isotopic compositions were corrected using the appropriate fractionation factors between CO_2 and H_3PO_4 to obtain the ''true'' $\delta^{13}C$ and $\delta^{18}O$ values of the carbonates. Isotopic composition of CO_2 is reported in units of ‰ relative to Pee Dee belemnite (V-PDB; see Kyser 1987). Replicate analyses are reproducible to ± 0.1‰ for both $\delta^{18}O$ and $\delta^{13}C$ values (Table 1).

Ion Microprobe Stable Isotopic Analyses

Ion microprobe samples were prepared by cutting and mounting portions of polished thin-section from NCL core in epoxy resin alongside polished grains of calcite, dolomite, and Fe-dolomite standards. A gold coat 200 Å thick was sputter-deposited on the sample mount surface prior to analysis.

←

FIG. 2.—Generalized stratigraphic section through the San Joaquin basin in the vicinity of the North Coles Levee. An expanded section of the Stevens sands shows the dolomite and calcite cement zones. Also shown is an expanded section through a typical calcite and dolomite cement zone from well 488–29 from North Coles Levee. The calcite cement zones generally consist of 95% calcite, by volume, whereas the dolomite cement zones consist mainly of dolomite ($\sim$ 65–70%) but may contain up to 10–15% calcite and 10% Fe-dolomite. The stratigraphy of the San Joaquin basin in the vicinity of the North Coles Levee is shown in the upper left. Abbreviations: Ss = uncemented Stevens sandstone; Cc = calcite cement zone; Do = dolomite cement zone.

TABLE 2.—*Mineralogical, chemical, and isotopic composition of carbonate minerals, and calculated cement formation temperatures from the North Coles Levee, San Joaquin Basin*

Sample No.	Depth (m)	Mineral	CaO (wt%)	FeO (wt%)	MgO (wt%)	MnO (wt%)	$\delta^{18}O_{PDB}$ (‰)	$\delta^{13}C_{PDB}$ (‰)	**Temp. (°C) *$\delta^{18}O_{H20} = 0$	**Temp. (°C) *$\delta^{18}O_{H20} = 4$
488-29	2665	Calcite	54.57	1.73	0.86	1.76	−9.5 ± 0.5		67 ± 4	99 ± 5
			54.17	1.85	1.04	2.00	−8.6 ± 0.5		61 ± 3	91 ± 4
			53.47	1.43	0.77	1.69				
			51.41	1.58	0.71	1.44				
			53.00	1.42	0.71	1.36				
			52.23	1.47	0.72	1.66	−7.9 ± 0.5	−6.0 ± 0.7	56 ± 3	85 ± 4
			51.10	1.80	0.88	1.75	−8.0 ± 0.5	−6.5 ± 0.7	56 ± 3	86 ± 4
			53.00	1.45	0.70	1.74	−7.2 ± 0.7	−8.5 ± 0.7	51 ± 3	79 ± 4
			52.07	1.67	0.82	2.03				
			51.53	1.94	0.91	2.58	−8.3 ± 0.5	−7.7 ± 0.7	58 ± 3	88 ± 4
			53.65	1.90	0.96	1.91	−8.0 ± 0.5	−6.8 ± 0.7	56 ± 3	85 ± 4
			53.77	1.91	0.79	2.50	−7.6 ± 0.5		54 ± 3	82 ± 4
			53.10	2.21	1.03	2.05	−8.0 ± 0.5	−5.1 ± 0.7	57 ± 3	86 ± 4
			53.92	1.76	0.81	1.73	−8.2 ± 0.5		58 ± 3	87 ± 4
			56.86	1.47	0.58	1.57				
			55.06	1.55	0.69	1.95				
			53.78	1.61	0.71	1.81				
			54.78	1.61	0.66	1.62				
488-29	2720	Calcite	51.87	1.80	0.88	0.76				
			52.28	2.11	1.03	0.82				
			52.53	2.15	1.10	0.66				
			52.90	2.07	1.00	0.78				
			50.75	1.62	1.39	3.34	−8.4 ± 0.5	−7.6 ± 0.7	59 ± 3	89 ± 4
			49.76	1.76	1.57	3.26	−8.4 ± 0.5	−9.4 ± 0.7	59 ± 3	89 ± 4
			49.29	1.68	1.57	3.44	−8.8 ± 0.5		62 ± 3	93 ± 4
			48.98	1.61	1.57	3.23	−9.0 ± 0.5		63 ± 3	94 ± 4
			51.36	1.48	1.36	3.51	−9.1 ± 0.5		64 ± 3	95 ± 4
			50.62	1.80	1.51	3.57				
			50.01	1.68	1.37	3.59				
			49.69	1.65	1.40	3.45				
488-29	2720	Early Dolomite	30.90	5.55	18.51	0.20	4.4 ± 0.6		7 ± 2	25 ± 2
			30.88	5.39	19.41	0.20	2.2 ± 0.6	6.2 ± 0.7	17 ± 2	36 ± 2
			30.73	5.25	19.40	0.16	3.4 ± 0.6	7.3 ± 0.7	11 ± 2	30 ± 2
			30.68	5.19	19.45	0.18	3.9 ± 0.6	7.4 ± 0.7	9 ± 2	27 ± 2
			30.26	5.29	19.56	0.21	3.2 ± 0.6	8.2 ± 0.7	12 ± 2	31 ± 2
			30.34	5.46	19.56	0.16	3.7 ± 0.6	10.7 ± 0.7	10 ± 2	28 ± 2
			31.30	5.25	19.50	0.17	4.1 ± 0.6	10.8 ± 0.7	9 ± 2	26 ± 2
			30.15	5.97	19.86	0.16	3.5 ± 0.6	10.3 ± 0.7	11 ± 2	29 ± 2
			31.13	4.72	19.97	0.24	4.4 ± 0.6	8.9 ± 0.7	7 ± 2	25 ± 2
			30.16	5.86	19.34	0.16	4.6 ± 0.6	11.5 ± 0.7	6 ± 2	24 ± 2
			30.13	5.27	19.50	0.19	4.4 ± 0.6		7 ± 2	25 ± 2
			30.52	7.81	17.74	0.31	4.3 ± 0.6	10.9 ± 0.7	8 ± 2	26 ± 2
			30.91	5.52	18.54	0.14	3.6 ± 0.6	10.3 ± 0.7	11 ± 2	29 ± 2
			30.13	4.92	20.63	0.20				
			30.35	4.85	19.61	0.20				
			30.49	5.38	19.64	0.15				
			30.52	5.67	19.76	0.18				
488-29	2780	Early Dolomite	30.51	7.53	17.80	0.24				
			30.62	7.94	17.74	0.19				
			30.36	7.62	17.96	0.24				
			30.62	8.08	18.00	0.31				
			30.62	7.86	17.93	0.21				
			31.22	7.77	17.62	0.18	2.8 ± 0.6	8.1 ± 0.7	14 ± 2	32 ± 2
			31.01	8.75	16.75	0.35	4.2 ± 0.6		8 ± 2	25 ± 2
			30.54	7.20	17.74	0.24	3.6 ± 0.6	7.4 ± 0.7	11 ± 2	29 ± 2
			28.74	9.48	17.77	0.19				
			29.41	8.68	17.71	0.17				
			29.94	7.59	18.05	0.24	2.8 ± 0.6		14 ± 2	32 ± 2
			28.72	9.20	17.68	0.24	3.4 ± 0.6		11 ± 2	29 ± 2
			30.67	7.70	17.71	0.16	2.0 ± 0.6	7.5 ± 0.7	17 ± 2	37 ± 2
			30.21	7.69	18.00	0.33	3.1 ± 0.6		13 ± 2	31 ± 2
			30.82	7.94	17.60	0.30				
488-29	2720	Fe-dolomite	33.53	11.35	9.32	3.37				
			31.51	12.40	9.73	4.09				
			32.27	11.66	9.47	4.29				
			33.41	10.36	13.23	0.67	−6.8 ± 0.9	−6.9 ± 0.4	70 ± 5	103 ± 7
			33.84	10.30	13.16	0.59	−6.1 ± 0.9	−5.6 ± 0.4	65 ± 5	97 ± 7
			32.88	10.54	13.00	0.66				
			33.86	10.28	13.04	0.55				
			33.09	10.66	13.31	0.70				
			28.66	11.71	14.56	1.53				
			29.57	11.02	15.51	1.66				
			28.94	11.10	16.35	1.36				

TABLE 2.—*Continued.*

Sample No.	Depth (m)	Mineral	CaO (wt%)	FeO (wt%)	MgO (wt%)	MnO (wt%)	$\delta^{18}O_{PDB}$ (‰)	$\delta^{13}C_{PDB}$ (‰)	**Temp. (°C) *$\delta^{18}O_{H20} = 0$	**Temp. (°C) *$\delta^{18}O_{H20} = 4$
488-29	2780	Fe-Dolomite	33.31	14.19	9.56	1.31				
			32.68	13.94	10.30	1.02				
			30.02	16.08	11.59	1.12				
			32.09	14.16	10.01	1.26				
			30.00	12.75	12.22	0.43				
			33.35	11.21	12.07	0.26	-6.9 ± 0.9		71 ± 5	104 ± 7
			33.66	11.49	11.87	0.32	-7.2 ± 0.9		73 ± 5	107 ± 7
			33.84	11.61	11.68	0.32	-7.4 ± 0.9		74 ± 5	109 ± 7
			33.45	11.02	12.09	0.38	-7.3 ± 0.9		73 ± 5	108 ± 7
			33.50	11.66	12.31	0.33	-7.0 ± 0.9		71 ± 5	104 ± 7
			33.07	14.33	9.33	1.18	-6.4 ± 0.9		67 ± 5	99 ± 7
			32.74	14.75	9.84	1.46	-6.3 ± 0.9	1.0 ± 0.4	67 ± 5	99 ± 7
			29.79	16.87	10.98	1.59	-6.3 ± 0.9		67 ± 5	99 ± 7
			33.93	12.13	11.58	0.38	-6.6 ± 0.9		69 ± 5	101 ± 7
			33.65	12.06	11.75	0.29	-6.9 ± 0.9		71 ± 5	104 ± 7
488-29	2780	Siderite	6.69	43.91	12.96	0.61				
			6.77	42.81	11.27	0.30				
			4.43	45.07	10.85	0.61				
			5.58	45.16	11.94	0.58				
			9.20	42.10	13.56	0.39				

* Oxygen isotopic composition of pore water is reported relative to SMOW in per mil.
** Errors on temperatures were calculated using the formula: $\sigma_T = (1/(2.78 \times 10^6)^{1/2}/(\delta\ ^{18}O_{sample}\text{-}\delta^{18}O_{H20} + 3.39)^{3/2})\sigma\delta^{18}O_{sample}$ (Mahon et al. 1998b).
Abbreviations: Temp. = temperature; No. = number.

In situ stable isotopic measurements were made at University of California, Los Angeles using the CAMECA ims 1270 ion microprobe (de Chambost et al. 1991) in multi-collection mode by sputtering with a ~ 20 μm $\times$ 25 μm, 0.5 nA primary beam of Cs^+ ions with impact energy of $\sim$ 20 keV. There are no thermal haloes associated with the sputtering process, and the depth of the sputtered pit is generally less than 3 μm. A normal-incidence electron flood gun was used to neutralize buildup of positive charge in the analysis area (Slodzian et al. 1987), and low-energy (0 to 30 eV) negative secondary ions were analyzed. A mass resolving power (M/ΔM) of $\sim$ 2000 (full width at 10% full height) was sufficient to eliminate isobaric hydride interferences. At this resolution, the contribution to the measurement of the minor isotope from the tail of the interference is estimated to be $<$ 0.1‰.

Carbon and oxygen isotopes were measured during separate analysis sessions. Oxygen isotopes were collected using Faraday cups (FC); the $^{16}O^-$ beam intensity was typically $\sim$ 80 pA. The FC signals were measured by electrometers housed in a temperature-controlled vacuum chamber ($\sim 10^{-3}$ torr) with a feedback resistor of 10^{11} Ω. Typically, drift in the FC detection system over a 12 hour period was $\sim$ 0.2 fA, or approximately 1‰ of the $^{18}O^-$ signal, and was corrected for by making several FC background measurements during each day of analysis. Measurements comprised 25 cycles, with each cycle consisting of a 10 s measurement. Internal precision of $\pm$ 0.3‰ under these conditions was routinely obtained for analyses of $\sim$ 5 minutes duration.

Carbon isotopes were collected using a FC detector for $^{12}C^-$ and an electron multiplier (EM) for ^{13}C. All other analytical conditions are as described above. Typically, $^{12}C^-$ beam intensities were $\sim$ 0.5 pA. The internal precision of single analyses was comparable to that for oxygen isotope measurements.

TABLE 3.—*Estimated temperature history of the Stevens sands, San Joaquin Basin*

Time (Ma) (Ma)	Depth (m)	Temperature °C
7	0	20
6	305	33
5	805	51
4	1305	68
3	1655	80
2	1855	87
1	1955	92
0	2005	95

Data from Mahon et al. (1998a).

The reproducibility between analyses on different spots of standards and unknowns (i.e., external reproducibility) with this technique depends primarily on (1) the stability of the EM counting efficiency for mixed detector (EM/FC) measurements, and (2) the stability of the electric potential in the analysis area, which is a function of the stability of the normal-incidence electron flood gun. Figure 3A shows oxygen isotopic analyses of different spots of the optical calcite standard (MS1212G) made over a 48 hour analysis session. These data show some additional scatter beyond the internal precision; however, there is no trend within a single population with a standard deviation of 0.47‰. This value may be taken as representative of the overall point-to-point reproducibility of the method. Similar results were obtained for the dolomite standard (MD dolomite; Fig. 3B) and the Fe-dolomite standard (MS1319; Fig. 3C).

The accuracy of the multi-collector SIMS measurement was tested by using the optical calcite as a primary standard to correct instrumental mass fractionation and treating MM calcite as an ''unknown''. Ion microprobe measurements of 18 spots of MM calcite give an average $\delta^{18}O$ value of -2.1 ± 0.3‰ (Table 1), which agrees well with the value obtained by conventional analysis (-2.0 $\pm$ 0.1‰; Table 1).

For oxygen and carbon isotopic analyses of NCL carbonates, an additional complication arises for samples that have a different chemical composition (i.e., Ca, Fe, and Mg) than that of our isotopic standards. Previous ion microprobe oxygen isotopic analyses of carbonates have demonstrated that the instrumental mass fractionation (IMF) can vary widely depending on sample chemistry (i.e., Ca, Fe, and Mg) and analytical conditions of the analysis (e.g., Eiler et al. 1997; Valley et al. 1997; Leshin et al. 1998; Riciputi et al. 1998). Thus, it is necessary to apply an additional correction for these ''matrix effects'' in order to obtain accurate $\delta^{18}O$ and $\delta^{13}C$ values for samples of intermediate chemical composition relative to standards. We characterized the magnitude of matrix effects on the IMF along the dolomite–ankerite solid solution by comparing the measured values of $^{18}O^-/^{16}O^-$ to the accepted $^{18}O/^{16}O$ for three isotopic standards (Table 1). The results show an approximate 8‰ difference in IMF for samples that differ by $\sim$ 60 mol% Fe (Fig. 4). Isotopic measurements of the NCL samples were corrected for IMF by calibration on compositionally similar standard

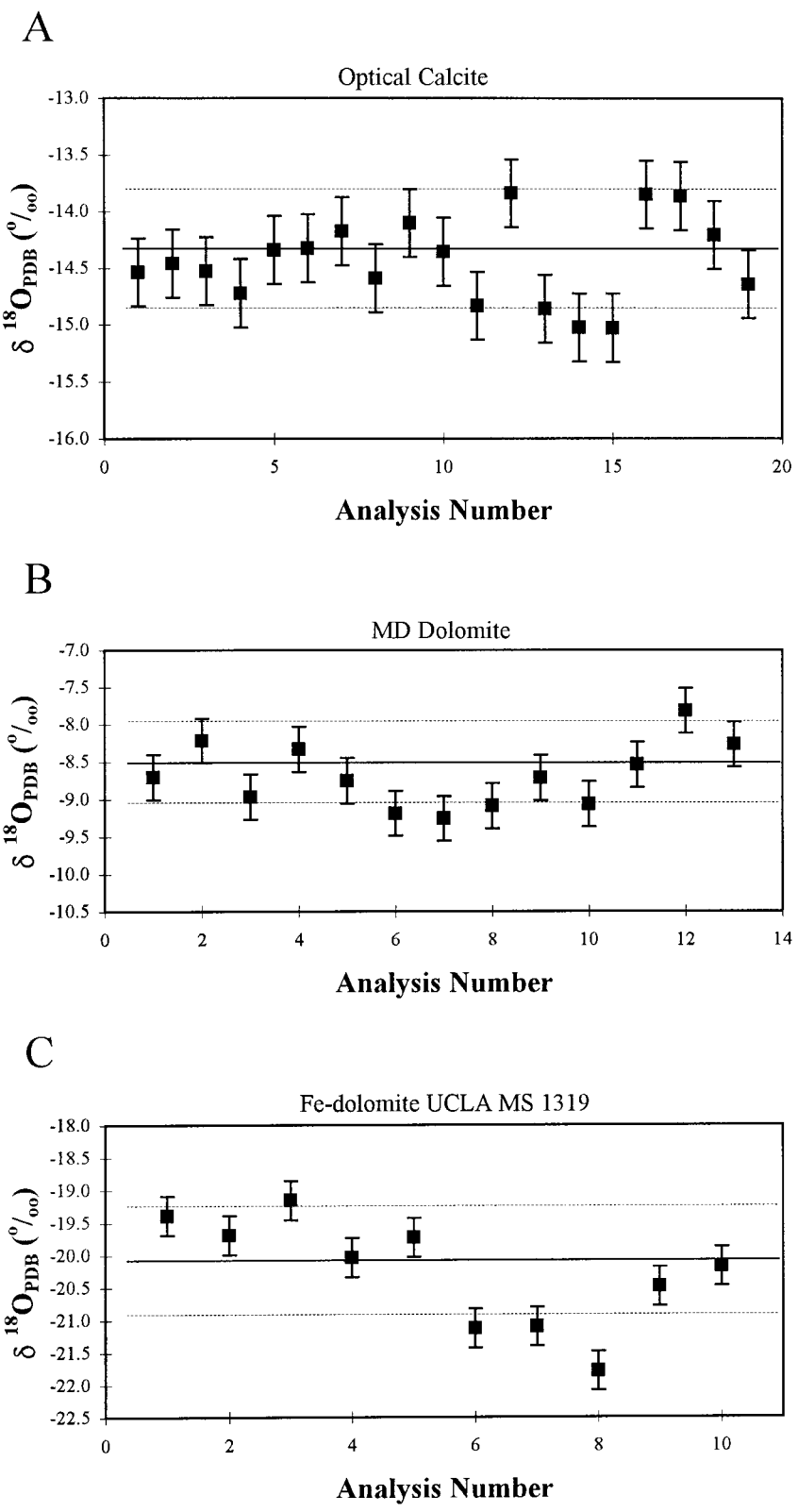

FIG. 3.—External reproducibility of oxygen isotope analyses of **A)** optical calcite, **B)** MD dolomite, and **C)** Fe-dolomite UCLA MS1319. Shown are mass-fractionation corrected $\delta^{18}O$ values with 1σ error bars. Dashed lines represent the standard deviation of the entire population.

carbonates measured during the same analysis session. Following isotopic analysis, the chemical composition of the carbonate was determined by electron microprobe analysis in and adjacent to the ion microprobe sputter pits. The chemical composition was used to correct the isotopic data for dolomite and Fe-dolomite for matrix effects by linearly interpolating the appropriate IMF obtained via analyses of standards (Fig. 4). Calcite from the NCL samples and our calcite standards were similar in composition, therefore corrections for matrix effects were negligible in this case.

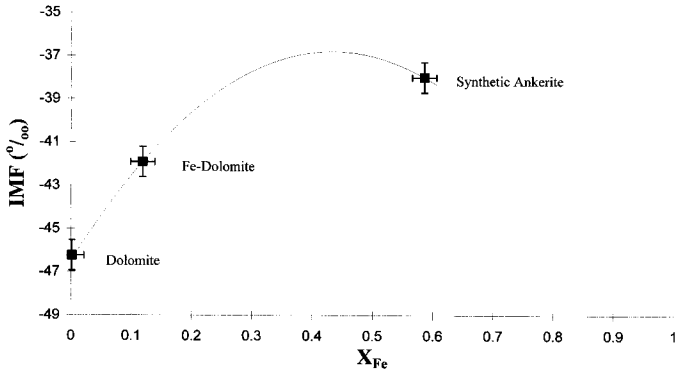

FIG. 4.—Instrumental mass fractionation (IMF), the difference in per mil between the measured and true $\delta^{18}O$ value, vs. chemical composition for carbonate minerals from the dolomite–ankerite solid solution (displayed as mole fraction of Fe in the minerals) used as standards for ion microprobe measurements. Each plotted data point represents the weighted mean (with standard error) of up to 21 analyses of each standard. As observed in previous ion probe studies of oxygen isotopes in carbonates, there is not a simple relationship between carbonate chemistry and IMF (Eiler et al. 1997; Valley et al. 1997; Leshin et al. 1998; Riciputi et al. 1998).

RESULTS

Petrographic Relations and Carbonate Mineral Paragenesis

The cement zones at NCL (Fig. 2) show a characteristic paragenetic sequence of early siderite followed by dolomite, calcite, and finally Fe-dolomite. Calcite is the most abundant cement phase and siderite is the least common (Boles 1998; this study).

Siderite (C1) occurs as scattered, small (10–15 μm), euhedral grains and clusters attached to detrital grains or enclosed by dolomite (Fig. 5A) and calcite. The siderite has a relatively Mg-rich composition (10.9 to 13.6 wt% MgO; Table 2) with up to 20 mole percent Mg relative to Fe (Fig. 6), probably reflecting the Mg-rich composition of marine water (Mozley 1989). Boles (1987) reported even higher Mg contents for siderite from NCL (up to 40 mole percent relative to Fe). However, these values are similar to the Mg contents of late Fe-dolomite (see below) and therefore may have been incorrectly reported as siderite.

Early Dolomite (C2) accounts for 30–40% of the sandstone volume in cemented zones and is therefore the most important early cement at NCL. Dolomite-cemented zones at NCL are generally found at depths below 2700 m and can reach up to 100 cm in thickness. These zones can be correlated laterally, in closely spaced drill core, for at least 120 m (Boles and Ramseyer 1987; Boles 1998). In thin section, early dolomite occurs as euhedral rhombs (up to 200 μm) enclosed by later Fe-dolomite (Fig. 5C) and less commonly by calcite. Early dolomite at 2720 m is characterized by low MnO contents ($<$ 1 wt %), FeO contents between 4.7 and 6.0 wt %, and MgO contents between 18.5 and 20.6 wt % (Fig. 7A; Table 2), similar to stoichiometric dolomite with MgO contents of $\sim$ 21 wt% (Deer et al. 1985). Early dolomite at greater depths ($>$ 2780 m) is also characterized by low MnO contents ($<$ 1 wt %; Fig. 7B; Table 2); however, this dolomite has higher FeO contents (7.2–9.5 wt %; Fig. 7A) and lower MgO contents (16.8–18.1 wt %; Fig. 7B; Table 2). Evidence for an early origin of dolomite includes high intergranular cement volume, euhedral rhomb-shaped crystals indicating precipitation into open pore space, alignment of cement zones parallel to bedding, and deformation of cement zones, suggesting early crystallization prior to compaction and folding (Boles and Ramseyer 1987).

Calcite (C3) cement is the most common cement type at NCL. In thin section, calcite occurs as interlocking mosaic of crystals (10–100 μm) that fill pore space (Fig. 5D) and occasionally replace detrital grains of plagioclase. Previous studies (Boles and Ramseyer 1987; Mahon et al. 1998b; Boles 1998) have shown, on the basis of variable isotopic compositions, that there are two calcite cementation events, whereas other studies have shown that there is little variation among calcite-cemented zones in the central basin (e.g., Schultz et al. 1989). We have identified two populations of calcite cement at NCL on the basis of stratigraphy, element chemistry, and isotopic composition. Samples from a depth of 2665 m are completely cemented by calcite, whereas dolomite and Fe-dolomite are absent. This calcite is characterized by CaO contents between 51.1 and 56.9 wt % (Fig. 8A; Table 2) and low MgO (0.6–1.1 wt %; Fig. 8B; Table 2) and MnO contents (0.7–2.6 wt %; Fig. 8A; Table 2). A second but subordinate population of calcite cement occurs at deeper stratigraphic levels (2720 m) in association with dolomite and Fe-dolomite. This calcite is characterized by lower CaO contents (49.0–51.4 wt %; Fig. 8A; Table 2) and higher MgO (1.4–1.6 wt %; Fig. 8B; Table 2) and MnO contents (3.2–3.6 wt %; Fig. 8A; Table 2) relative to the dominant calcite cements. Both calcite populations have similar but variable FeO contents (Table 2), postdate dolomite, and precede the precipitation of Fe-dolomite.

Fe-dolomite (C4) is intimately associated with early dolomite and occurs as a mosaic of interlocking crystals (5–50 μm) that fill pore space between early dolomite rhombs (Fig. 5B) and within cleavage spaces of crushed detrital biotite, and replaces early dolomite (Fig. 5C). Biotite associated with Fe-dolomite is partially altered to phlogopite. In biotite-rich zones that are cemented by early dolomite, Fe-dolomite represents up to 50% of the cement. The Fe-dolomite has variable chemical compositions relative to early dolomite, but is characterized generally by higher FeO (11.0–16.9 wt % ; Fig 9A) and MnO contents (0.3–4.3 wt %; Fig. 9B) and lower MgO (9.3–16.4 wt %; Fig. 9A) and CaO contents (28.7–33.9 wt %; Fig. 9C). On the basis of petrographic relations, Fe-dolomite is relatively late. In addition, Fe-dolomite's variable chemical compositions and association with altered biotite and feldspar suggest that Fe-dolomite formed as a product of late fluid–rock interaction. The iron in this dolomite was likely derived from the breakdown of biotite, feldspar, and early dolomite by the reaction

$$\underset{\text{(biotite)}}{K(Fe, Mg)_3(Fe, Al)Si_3O_{10}(OH)_2} + \underset{\text{(dolomite)}}{3CaMg(CO_3)_2} + \underset{\text{(fluid)}}{3CO_2} + \underset{\text{(from feldspar)}}{Al_2O_3}$$
$$= \underset{\text{(Fe-dolomite)}}{3CaMgFe(CO_3)_2} + \underset{\text{(phlogopite)}}{K(Mg)_3AlSi_3O_{10}(OH)_2} \quad [1]$$

Similar observations have been reported for the Wilcox Group, Texas Gulf Coast, where late ankerite cement formed from pre-existing calcite at temperatures of 120–160°C (Boles 1978, 1981, 1982).

Stable Isotopic Analyses

Dolomite, Fe-dolomite, and calcite cements (Table 2) were analyzed by ion microprobe in multi-collection mode. Early dolomite has a range of $\delta^{18}O$ values between +2.0‰ to +4.6‰ (Fig. 10A; Table 2) and $\delta^{13}C$ values between +6.2‰ and +11.5‰ (Fig. 10B; Table 2). The low $\delta^{13}C$ values ($\sim$ +6.2‰) are from early dolomite that was partially altered to Fe-dolomite. The least altered early dolomite has the highest $\delta^{13}C$ values (+10.3‰ to +11.5‰; Fig. 10A; Table 2). Although early dolomite in the sample from 2720 m is chemically distinct from early dolomite in the sample from 2780 m (i.e., high FeO contents; 7.2–9.5 wt %; Fig. 7A and low MgO contents; 16.8–18.1 wt %; Fig. 7B; Table 2), early dolomite shows little variation in $\delta^{18}O$ and in $\delta^{13}C$ values. All samples of early dolomite have positive $\delta^{18}O$ and $\delta^{13}C$ values and therefore are distinctive from Fe-dolomite and calcite, which have much lower $\delta^{18}O$ and $\delta^{13}C$ values (Fig. 11; Table 2).

Previous studies that used bulk acid dissolution techniques for stable isotopic analyses of carbonate cements from North Coles Levee (Boles and Ramseyer 1987; Wood and Boles 1991; Boles 1998) showed that early dolomite has $\delta^{18}O$ values that range from −3.5‰ to 0‰ and $\delta^{13}C$ values

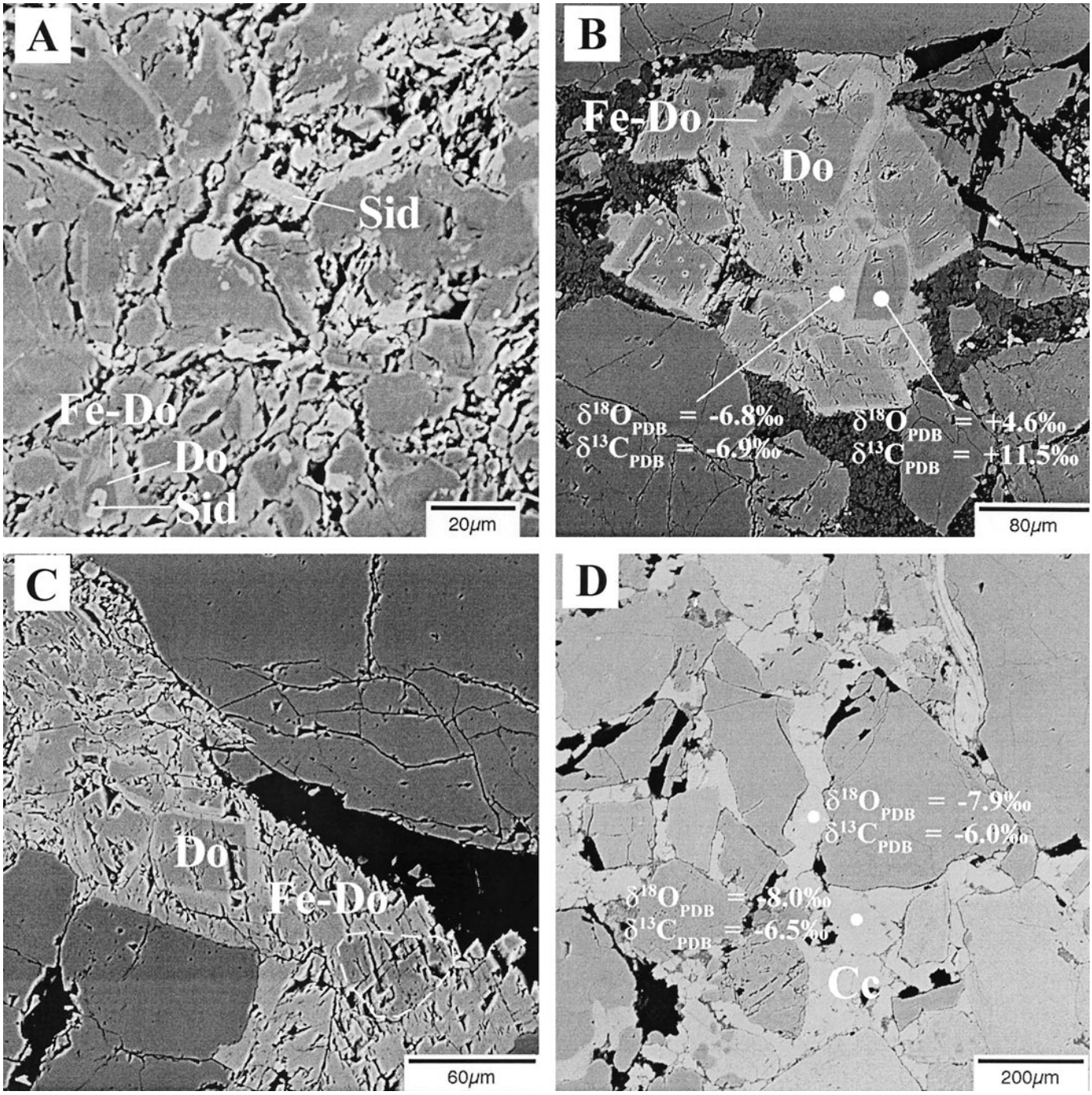

FIG. 5.—Back-scattered electron photographs of carbonate cements from North Coles Levee oil field. **A)** Sample (488–29; 2780 m) showing siderite (Sid), early dolomite (Do), and late Fe-dolomite (Fe-Do). **B)** Sample (488–29; 2780 m) showing partially altered early euhedral dolomite (Do) in a matrix of late Fe-dolomite. **C)** Sample (488–29; 2780 m) showing highly altered early euhedral dolomite (Do) in a matrix of late Fe-dolomite. Dashed line outlines a grain of early dolomite that is almost entirely altered to Fe-dolomite. White dots represent spots analyzed for their $\delta^{18}O$ values and $\delta^{13}C$ values (shown). **D)** Sample (488–29; 2665 m) showing calcite cements (Cc). White dots represent spots analyzed for their $\delta^{18}O$ values and $\delta^{13}C$ values (shown). Data from Table 2.

from +4‰ to +10‰. The relatively low $\delta^{18}O$ and $\delta^{13}C$ values obtained by bulk acid dissolution techniques are likely due to analyses of mixed dolomite phases (i.e., early dolomite with high $\delta^{18}O$ and $\delta^{13}C$ values and late Fe-dolomite with low $\delta^{18}O$ and $\delta^{13}C$ values) because the bulk $\delta^{18}O$ and $\delta^{13}C$ values are approximately the average of the *in situ* results (Fig. 11).

Calcite cements have a restricted range of $\delta^{18}O$ values (-9.9‰ to −7.2‰; Fig. 10A; Table 2) and $\delta^{13}C$ values between −9.4‰ and −5.1‰ (Fig. 10B; Table 2). These values are similar to results obtained by Wood and Boles (1991; Fig. 11) and Mahon et al. (1998b). All calcite samples have negative $\delta^{18}O$ and $\delta^{13}C$ values and therefore are distinctive from Fe-dolomite and early dolomite, which have relatively higher $\delta^{18}O$ and $\delta^{13}C$ values (Fig. 11; Table 2). Calcite cements that occur at depths of ~ 2665 m and are characterized by relatively high CaO contents and low MgO and

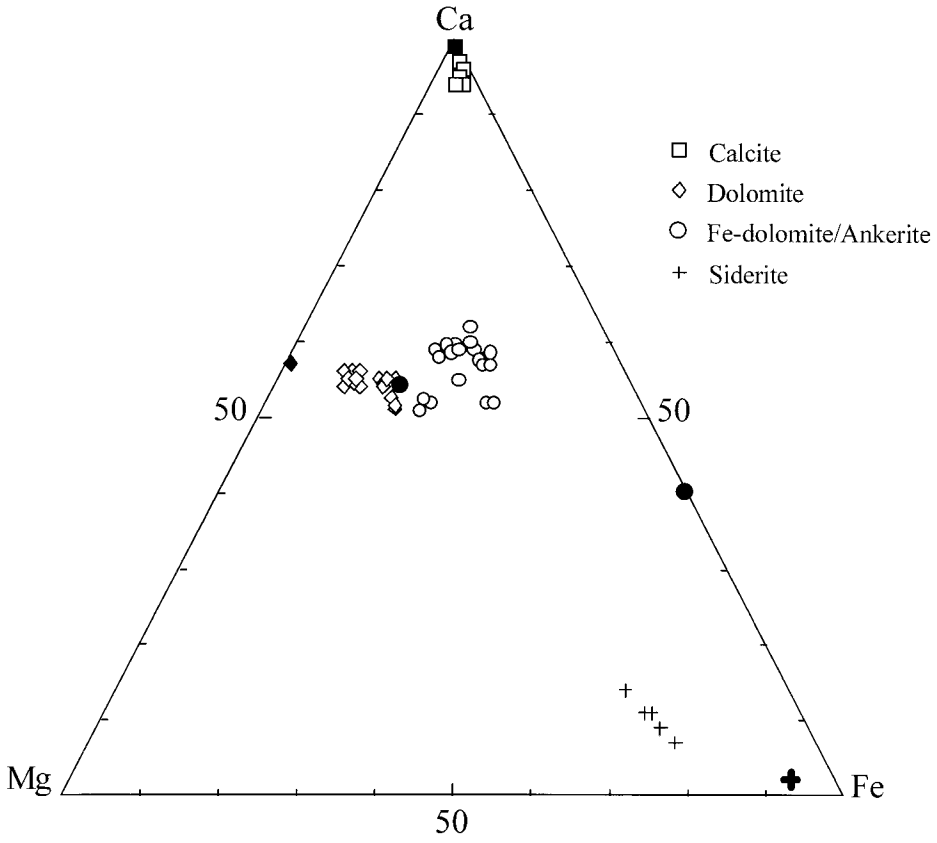

FIG. 6.—Mole proportions of Ca, Fe, and Mg in North Coles Levee cements (open symbols) and standards (closed symbols). Data calculated from data in Tables 1 and 2.

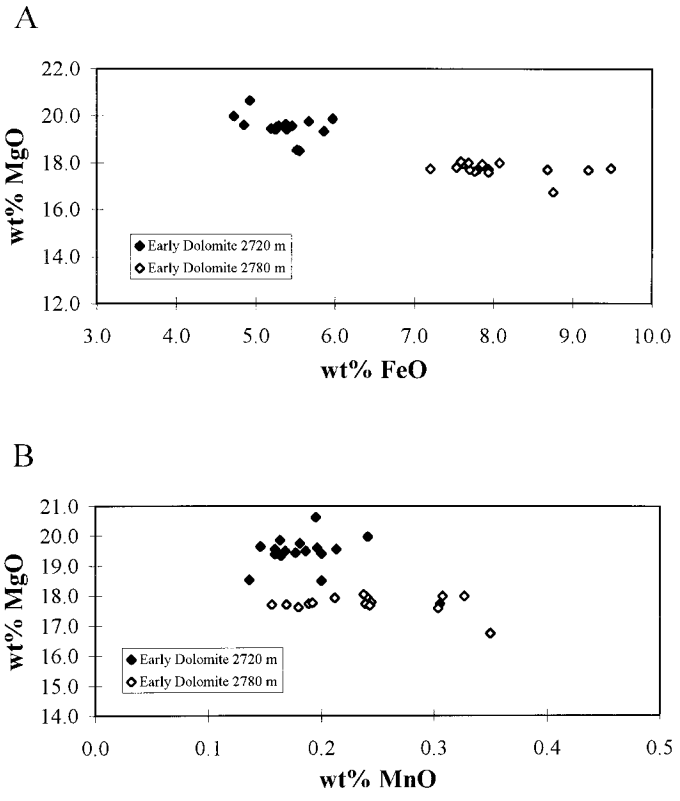

FIG. 7.—Relationship between **A)** MgO and FeO, and **B)** MgO and MnO for early dolomite. Data from Table 2.

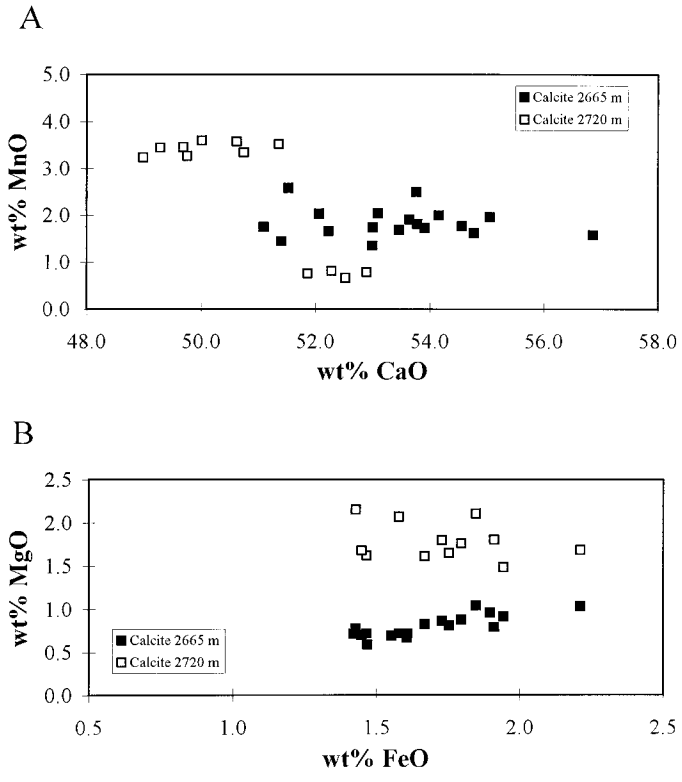

FIG. 8.—Relationship between **A)** MnO and CaO, and **B)** MgO and FeO for calcite. Data from Table 2.

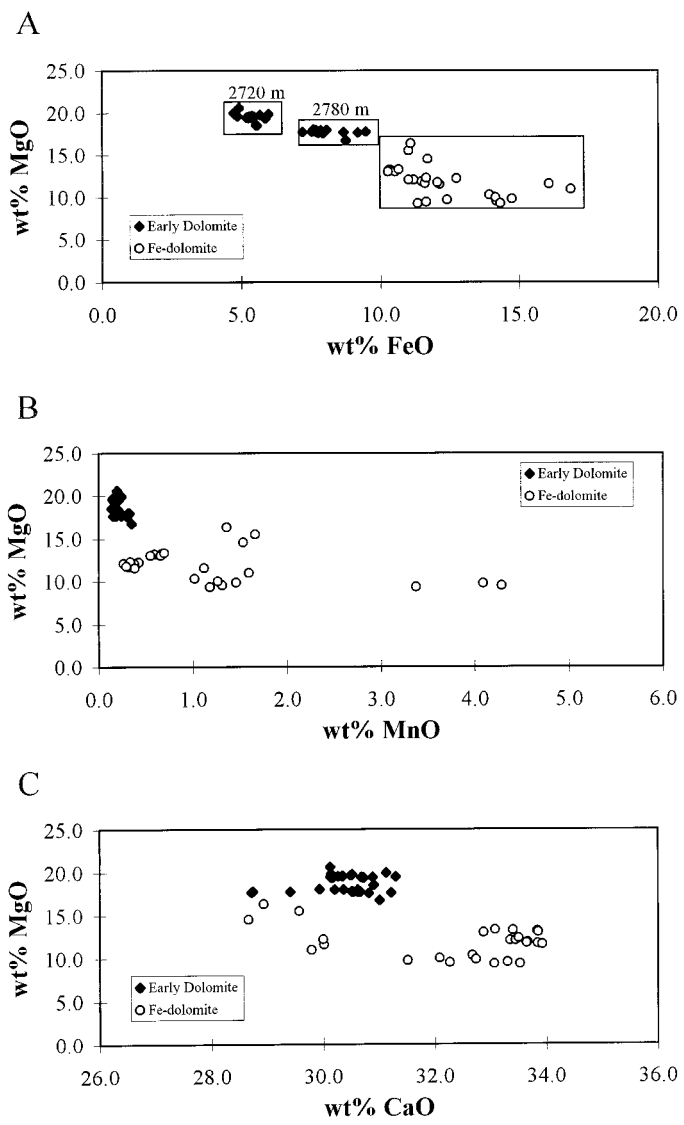

FIG. 9.—Relationship between **A)** MgO and FeO, **B)** MgO and MnO, and **C)** MgO and CaO for early dolomite and Fe-dolomite. Data from Table 2.

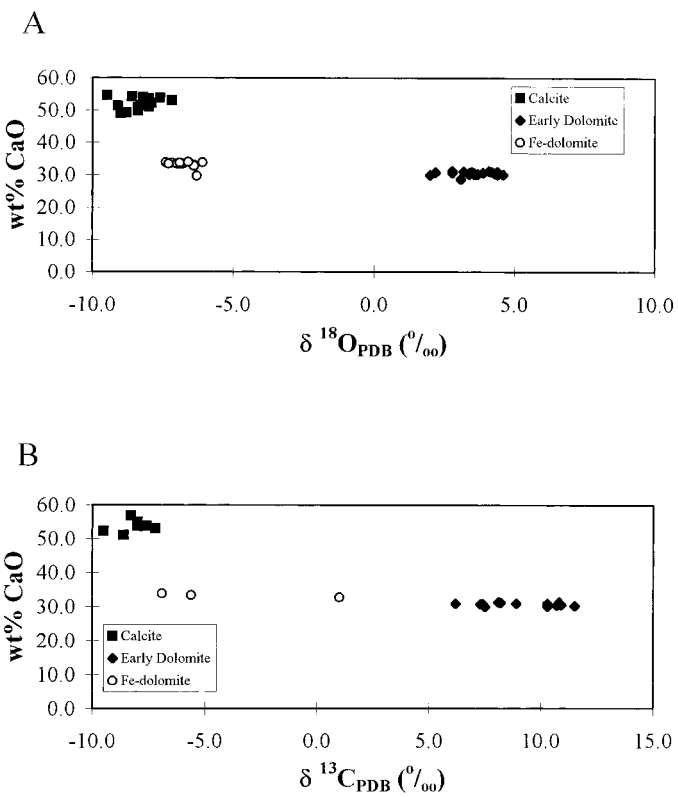

FIG. 10.—Relationship between **A)** CaO and $\delta^{18}O$ values, and **B)** CaO and $\delta^{13}C$ values, for calcite, early dolomite, and Fe-dolomite. Symbol size is indicative of 1σ error. Data from Table 2.

MnO contents (Table 2) have slightly higher $\delta^{18}O$ and $\delta^{13}C$ values (Fig. 12A, B; Table 2) relative to calcite cements that occur at deeper stratigraphic levels (2720 m), which are characterized by lower CaO contents and higher MgO and MnO contents (Table 2). In addition, calcite cements generally have higher MnO contents and lower $\delta^{18}O$ values relative to Fe-dolomite (Fig 11C), suggesting that calcite cements and Fe-dolomite formed from two distinct fluids.

Fe-dolomite, which is paragenetically late, has a range of $\delta^{18}O$ values from $-6.3‰$ to $-7.4‰$ (Fig. 10A; Table 2) and $\delta^{13}C$ values between $-6.9‰$ and $+1.0‰$ (Fig. 10B; Table 2). The wide range in $\delta^{18}O$ and $\delta^{13}C$ and largely negative values for Fe-dolomite (Fig. 10A, B) reflect the variable alteration of early dolomite, which has high $\delta^{18}O$ and $\delta^{13}C$ values, by a late fluid with lower $\delta^{13}C$ values.

DISCUSSION

Paleotemperatures

The oxygen isotopic composition of carbonate cements can be used to estimate the temperature of carbonate precipitation (e.g., the calcite-H_2O thermometer; Friedman and O'Neil 1977). This requires knowledge of the oxygen isotopic composition of both the carbonate phase and the pore-water in equilibrium with the carbonate. The chief uncertainty in this approach relates to the pore-fluid composition. While the initial composition of the pore fluid in marine sands is likely to be similar to seawater, diagenetic reactions tend to enrich the fluid in ^{18}O (e.g., Clayton et al. 1966; Savin 1980; Anderson and Arthur 1983).

At North Coles Levee, the initial $\delta^{18}O_{SMOW}$ value of Miocene marine pore water is assumed to be 0‰ (Savin 1977; Woodruff et al. 1981), whereas the present measured value of pore water from the Stevens sands is $+4‰$ (Schultz et al. 1989; Fisher and Boles 1990). A variety of approaches can be applied to model pore-fluid evolution within the Stevens sands. Both Wood and Boles (1991) and Mahon et al. (1998b) calculated temperatures by assuming that the pore water evolved linearly from a $\delta^{18}O_{SMOW}$ value of 0‰ at $\sim 20°C$ to a $\delta^{18}O_{SMOW}$ value of $+4‰$. Mahon et al. (1998b) additionally calculated temperatures by assuming a constant value of pore water equivalent to late Miocene seawater (i.e., $\delta^{18}O_{SMOW} = 0‰$). Pore-water evolution generally involves clay mineral interaction or mixing with other fluids such as meteoric water (Clayton et al. 1966; Hitchon and Freidman 1969; Suchecki and Land 1983; Longstaffe 1987, 1994; Longstaffe et al. 1992). The Mahon et al. (1998b) model neglects clay mineral interactions capable of enriching pore fluids in ^{18}O because the burial temperatures required for oxygen isotopic exchange to occur between water and clay minerals (i.e., $> 100°C$; O'Neil and Kharaka 1976; James and Baker 1976; Savin and Yeh 1981; Longstaffe 1987, 1994; Longstaffe et al. 1992) have only recently been attained (i.e., 1–2 Ma) in the Stevens sandstone. In addition, there is no evidence for mixing between meteoric water and marine pore-water in the central San Joaquin basin because present-day meteoric water in the basin has a $\delta^{18}O_{SMOW}$ value of $-13.5‰$, which would produce pore water with a negative $\delta^{18}O_{SMOW}$ value. Taking these consid-

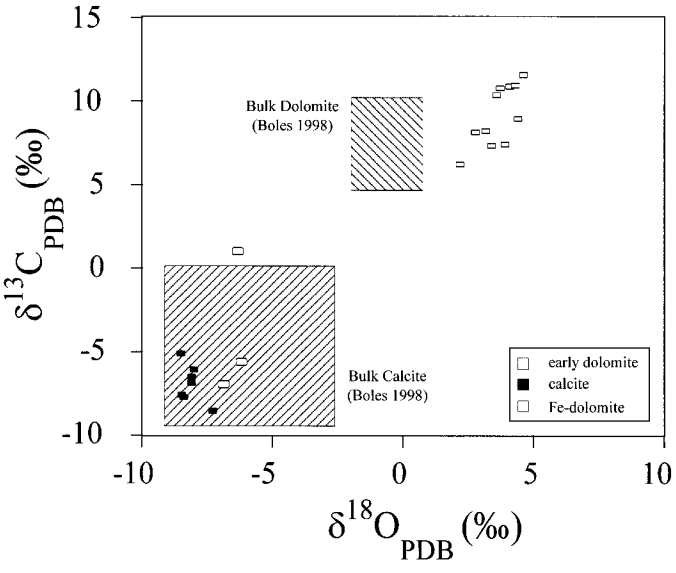

FIG. 11.—Relationship between $\delta^{18}O$ values and $\delta^{13}C$ values, for calcite, early dolomite, and Fe-dolomite. Symbol size is indicative of 1σ error. Data from Table 2.

erations into account, it seems likely that pore-water in the Stevens sandstone evolved linearly over time at temperatures far below 100°C (cf. Wood and Boles 1991; model II of Mahon et al. 1998b).

A more plausible model for pore-water evolution in the Stevens sandstone is that pore water initially had a $\delta^{18}O_{SMOW}$ value equivalent to late Miocene seawater (i.e., $\delta^{18}O_{SMOW} = 0‰$) and only recently (i.e., the past 2 My) was enriched in ^{18}O by water–rock interaction as temperatures approached 100°C. This is reasonable because presently much of the basin pore water has a salinity similar to sea water, but at deeper levels where temperatures exceed 100°C, the pore-water composition has been modified by reaction with plagioclase and organic matter, and contains an abundance of organic acids (Carothers and Kharaka 1978; MacGowen and Surdam 1988; Fisher and Boles 1990; Feldman et al. 1993). In the calculations below we assume that the $\delta^{18}O$ of pore fluid was constant at 0‰ from 7 to 2 My (5–90°C) and increased abruptly from 0‰ to 4‰ between 2 and 0 Ma (90–105°C).

Measured $\delta^{18}O$ values from early dolomite cements (Table 2) give precipitation temperatures of 10 ± 5°C using the dolomite–water fractionation factors of Fritz and Smith (1970) and a pore fluid composition of 0‰. Sediments comprising the North Coles Levee oil field were deposited in a deep marine setting (Callaway 1990) where bottom water temperatures likely ranged from $\sim$ 5°C to 10°C (Arrhenius 1957; Giambalvo et al. 1997). This suggests that early dolomite precipitated at or near the sediment–water interface soon after deposition (e.g., Carballo et al. 1987; James et al. 1993; Mazzullo et al. 1995). Note that temperatures for precipitation of early dolomite calculated by Boles and Ramseyer (1987) and Wood and Boles (1991) assuming linear increase in $\delta^{18}O$ of pore fluid with time are distinctly higher (34–48°C) than the values we calculate.

Assuming a $\delta^{18}O_{SMOW}$ value of 0‰ for the water and the oxygen isotope fractionation factor for calcite–water of Friedman and O'Neil (1977), calculated temperatures of precipitation for calcite cements are between 51°C and 67°C. These results suggest that calcite cement at North Coles Levee precipitated at ca. 5–4 Ma (Fig. 13A). If the model of Wood and Boles (1991) for pore fluid evolution is applied, calculated values for precipitation temperatures would be 15–20°C higher.

Measured $\delta^{18}O$ values for late Fe-dolomite cements give precipitation temperatures of 97–107°C using the fractionation factor of Fritz and Smith (1970) when a pore fluid $\delta^{18}O$ value of 4‰ is assumed. These temperatures are 65–73°C if the pore-fluid composition is assumed to be 0‰. Several

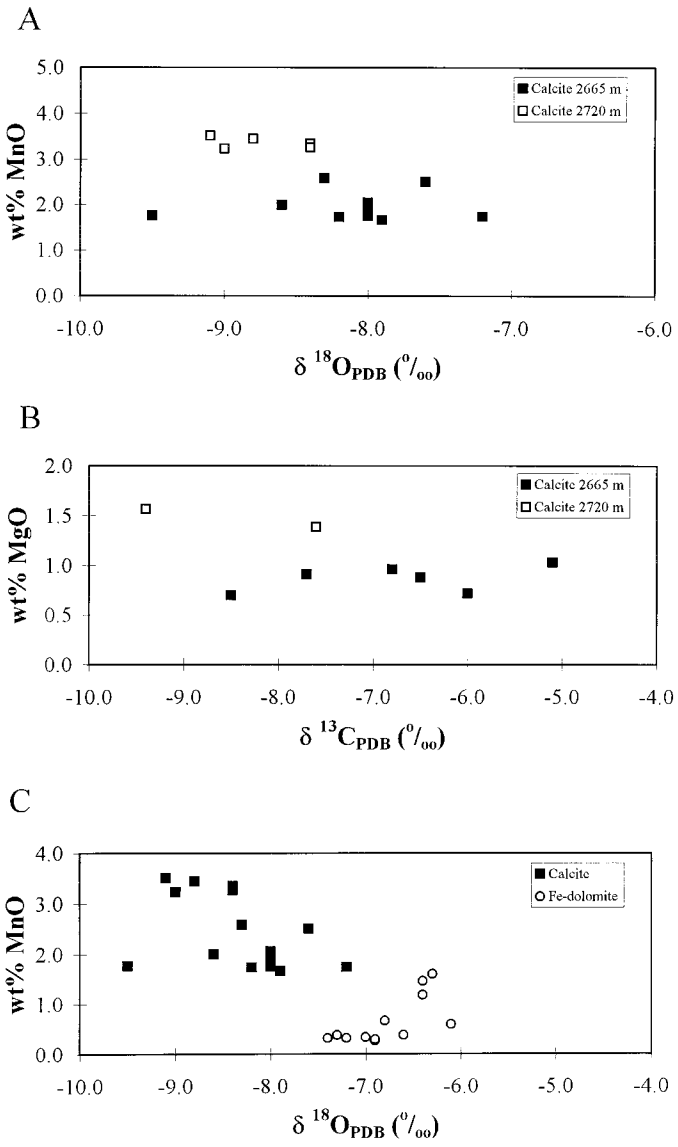

FIG. 12.—Relationship between **A)** MnO and $\delta^{18}O$ values, **B)** MgO and $\delta^{13}C$ values for calcite, and **C)** MnO and $\delta^{18}O$ values for calcite and Fe-dolomite. Symbol size is indicative of 1σ error. Data from Table 2.

lines of evidence cause us to favor temperatures calculated using present-day 4‰ value. Fe-dolomite is paragenetically late and generally found at depths greater than 2720 m, which is consistent with precipitation at higher temperatures. As described by Boles and Ramseyer (1987), association of Fe-dolomite with biotite alteration is more common in cores cut after 1965 (NCL 88–29, 487–29, 488–29) than in cores cut before 1960. This suggests that the bulk of Fe-dolomite formed within the past 35 years in response to reduced pore-water fluid pressure as the gas cap was removed at NCL (Boles and Ramseyer 1987).

Sources of Carbon

The isotopic composition of carbon in carbonate cements can be used to determine its source. The early dolomite cements have $\delta^{13}C$ values between $+6.2‰$ and $+11.5‰$, suggesting that they formed in a reducing environment where methane preferentially fractionates isotopically light carbon, leaving the pore fluid enriched in ^{13}C (Coleman et al. 1986). In contrast, the calcite cements have low $\delta^{13}C$ values between $-9.4‰$ and $-5.1‰$.

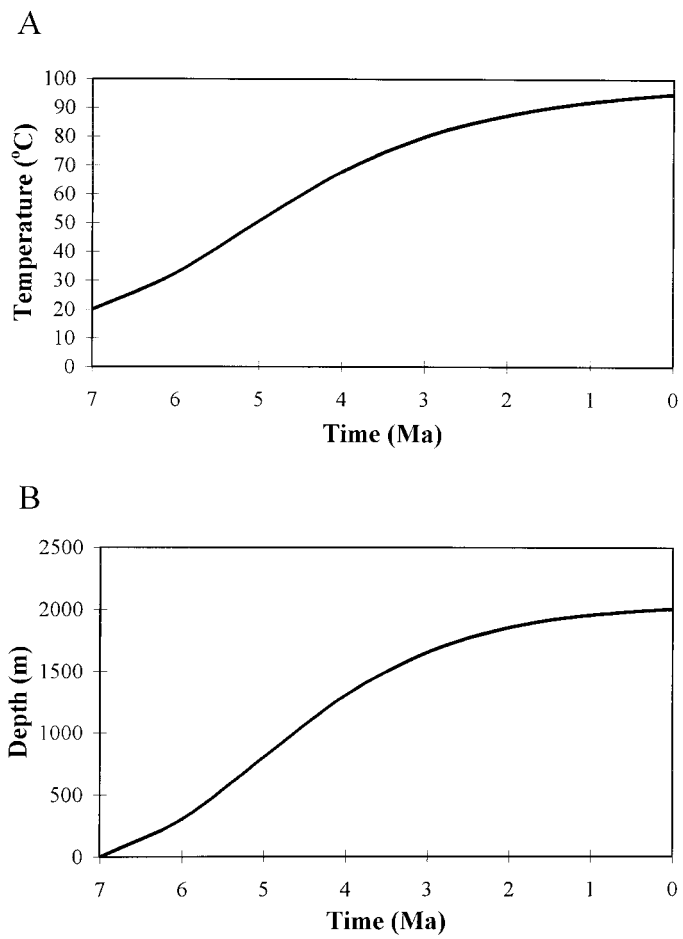

FIG. 13.—**A)** Temperature evolution predicted for the Stevens sands interval used in Mahon et al. (1998b). **B)** Burial history estimated for North Coles Levee oil field using data from Reid (1990). Data from Table 3.

In general, calcite precipitated from marine waters (i.e., detrital shell material) has a $\delta^{13}C \sim 0‰$, whereas calcite precipitated from the breakdown of hydrocarbons and kerogen (i.e. organic CO_2) has $\delta^{13}C$ values near $-20‰$ (Lundegard 1985; Wood and Boles 1991). Therefore, $\delta^{13}C$ values of the calcite cements at North Coles Levee are interpreted to represent a mixture of C from two sources: a source with a $\delta^{13}C$ value of $\sim 0‰$, such as detrital shell material, and organic carbon with a $\delta^{13}C$ value of $-20‰$. Fe-dolomite, which formed at the expense of early dolomite (Fig. 5C), has a wide range in $\delta^{13}C$ values between $-6.9‰$ and $+1.0‰$. These values represent a continuum between the high $\delta^{13}C$ values of early dolomite and the low $\delta^{13}C$ values of calcite (Fig. 10A, B) and likely represent a mixture of C from several sources, including detrital shell material, organic carbon, and early dolomite.

The negative $\delta^{13}C$ values of calcite reflect periods in which isotopically light CO_2 was produced and mixed with pore water. Large quantities of CO_2 would be produced when organic-rich shales such as the Kreyenhagen and Tumey formations passed through the CO_2 window (90–100°C; analogous to the oil window for hydrocarbons; Wood and Bole 1991). Therefore, the source of light carbon incorporated in the calcite cements at NCL was likely the Kreyenhagen and Tumey formations, because these formations would have been at a depth corresponding to those temperatures at the same time the calcite cements were precipitated (4–5 Ma, see below).

Thermal Evolution and Timing of Cementation

The temperature–depth–time model of Mahon et al. (1998a) was used in conjunction with the calculated temperatures of precipitation of carbonate cement to ascertain the timing of cementation at NCL. Early dolomite precipitated at temperatures near 10 ± 5°C, suggesting precipitation at ~ 7 Ma at or near the water–sediment interface. Boles (1998), however, using oxygen isotopic data obtained from analyses of bulk carbonates, suggested that dolomite precipitated at temperatures of 30–40°C, corresponding to a depth of 500–1000 m and time of cementation of 5–6 Ma. The cause of discrepancy is likely due to the bulk carbonate analyses including various proportions of early dolomite and late Fe-dolomite.

Calcite cements at North Coles Levee precipitated over a range of apparent temperatures between 51°C and 67°C, suggesting continuous precipitation between 5 Ma and 4 Ma over a depth range of 800–1300 m. Wood and Boles (1991) reported a similar timing of cementation for calcite at NCL. However, Mahon et al. (1998b), on the basis of preliminary results from the Elk Hills reservoir, concluded that calcite cementation occurred semi-continuously after deposition at 7 Ma and continued until about 3 Ma.

Fe-dolomite, assuming a pore water $\delta^{18}O_{SMOW}$ value of $+4‰$, precipitated (or is currently being precipitated) at temperatures of ~ 100°C at maximum burial depths of > 2000 m. These results are consistent with empirical and petrographic observations (i.e. an abundance of Fe-dolomite in cores cut after 1965 [NCL 88–29, 487–29, 488–29] relative to cores cut prior to 1960).

The Stevens sands were largely cemented by 5 Ma. Therefore, the source of the petroleum was likely interbedded shales (Mahon et al. 1998b). The Eocene Kreyenhagen and Tumey shales, which lie stratigraphically below the Stevens sands, reached depths corresponding to temperatures of 90–120°C (oil generation window; Hunt 1979) between 4 and 5 My. Therefore, these shales may in part have been the source of the petroleum at NCL because the early dolomite cements, already emplaced (7 Ma), may have restricted vertical fluid flow, thereby trapping migrating hydrocarbons. However, recent calculations of temperature history (Mahon et al. 1998a) suggest that the Stevens sands and other organic-rich shales proximal to the Stevens sands, such as the Monterey Formation, reached the oil generation window (90–120°C; Hunt 1979) at 1–2 Ma. Recent studies have also shown that the main source of liquid hydrocarbon extraction at NCL was likely organic rich sediments of the Monterey Formation that lie below and are in close proximity to the Stevens sands (Peters et al. 1994). However, the basin has abundant hydrocarbon accumulations that have resulted from organic diagenesis (Callaway 1971; Boles 1998). The oils are found throughout the stratigraphic sections, indicative of cross-formational flow from deeper levels in the basin (Boles 1998). Therefore, secondary hydrocarbon migration from pockets trapped by early dolomite cements may have occurred at 1–2 Ma and were re-trapped by the calcite cements, thus enhancing hydrocarbon accumulation at North Coles Levee.

CONCLUSIONS

1. Ion microprobe analysis in multi-collection mode permits rapid (i.e., < 5 minutes/analysis), precise ($\pm$ 0.5‰) *in situ* oxygen and carbon isotopic analysis of carbonates. This represents a three fold improvement in measurement efficiency and two fold improvement in precision over previous ion microprobe measurements performed with similar materials (Mahon et al. 1998b).

2. *In situ* measurements have allowed us to isotopically characterize multiple generations of carbonate cements that exhibit large variation in $\delta^{18}O$ values over very short distances (e.g., 12‰ contrast between early dolomite and late Fe-dolomite separated by ~ 20 μm, as shown in Fig. 4B). Integrating petrochemical observations with such measurements has permitted us to identify three main stages of carbonate cementation and to refine previous models (Boles and Ramseyer 1987; Wood and Boles 1991) for progressive carbonate cementation within the Stevens sands at NCL.

3. *In situ* oxygen and carbon isotopic analyses in conjunction with electron microprobe data show that early dolomite cements and calcite cements that form the majority of the cement zones at NCL have distinct and relatively homogeneous isotopic compositions. Early dolomite from two different stratigraphic horizons (2720 m and 2780 m) have $\delta^{18}O$ values between +2‰ and +5‰, whereas calcite cements from 2665 m and 2720 m depths have $\delta^{18}O$ values between −7‰ and −10‰. Paragenetically late Fe dolomite forming at the expense of early dolomite has $\delta^{18}O$ value of ~ −6.5‰.

4. The temperature, and by inference the timing, of carbonate cementation within the Stevens sands at NCL was estimated using the *in situ* oxygen isotope data, temperatures derived from equilibrium oxygen isotope fractionation factors for calcite–water and dolomite–water, and the temperature–depth–time model of Mahon et al. (1998a). These results suggest that carbonate cementation began with the precipitation of dolomite at or near the water–sediment interface (5–20°C) at ~ 7 Ma. Calcite cements were later precipitated at an intermediate stage (50–65°C) between ~ 4 Ma and 5 Ma at depths of 800 m to 1300 m. On the basis of petrographic observations and calculated model temperatures, Fe-dolomite likely precipitated very recently under present-day conditions (95–105°C). The cementation history described above is considerably more protracted than that indicated by previous studies that relied upon bulk carbonate analyses that were unable to distinguish early dolomite from late Fe-dolomite.

5. *In situ* carbon isotopic measurements show that carbon was likely derived from several sources: marine tests, hydrocarbons or kerogen, and a zone of methanogenesis.

ACKNOWLEDGMENTS

This study was supported by a grant from the Department of Energy (# 95 603036143W). We thank Dr. T.K. Kyser for providing the dolomite standard and the facilities for conventional isotopic analyses. Technical assistance was expertly provided by Kerry Klassen and Aliona Valyashko. We also thank Dr. Frank Kyte for his expert technical assistance. The UCLA ion microprobe laboratory is partially supported by a grant from the National Science Foundation Instrumentation and Facilities program. The manuscript benefited greatly for the reviews of Drs. Laura J. Crossey, Tracy D. Frank, Timothy W. Lyons, and David A. Budd.

REFERENCES

Anderson, T.F., and Arthur, M.A., 1983, Stable isotopes of oxygen and carbon and their application to sedimentologic and paleoenvironmental problems, *in* Arthur, M.A., Kaplan, I.R., Veizer, J., and Land, L.S., eds., Stable Isotopes in Sedimentary Geology: SEPM Short Course, 10, p. 111–151.

Arrhenius, G.S., 1957, Climatic records on the ocean floor, *in* Craig, H., ed., Conference on Recent Research in Climatology: University of California, San Francisco, p. 25–35.

Bent, J.V.B., 1988, Paleotectonics and provenance of Tertiary sandstones of the San Joaquin basin, California, *in* Studies of the Geology of the San Joaquin basin: SEPM, Los Angeles, California, p. 109–120.

Boles, J.R., 1978, Active ankerite cementation in the subsurface Eocene of south-west Texas: Contributions to Mineralology and Petrology, v. 68, p. 13–22.

Boles, J.R., 1981, Clay diagenesis and effects on sandstone cementation (case histories from the Gulf Coast Tertiary), *in* Longstaffe, F.J., ed., Clays and the Resource Geologist, Mineralogical Association of Canada, Short Course 7, p. 148–168.

Boles, J.R., 1982, Active albitization of plagioclase, Gulf Coast Tertiary: American Journal of Science, v. 282, p. 165–180.

Boles, J.R., 1987, Six million year diagenetic history, North Coles Levee, San Joaquin Basin, California, *in* Marshal, J.D., ed., Diagenesis of Sedimentary Sequences: Special Publication, Geological Society, London 36, p. 191–200.

Boles, J.R., 1998, Carbonate cementation in Tertiary sandstones, San Joaquin basin, California, *in* Morad, J.A., ed., Special Publication, International Association of Sedimentologists 26, p. 261–283.

Boles, J.R., and Ramseyer, K., 1987, Diagenetic carbonate in Miocene sandstone reservoir, San Joaquin basin, California: American Association of Petroleum Geologists, Bulletin 71, p. 1475–1487.

Callaway, D.C., 1971, Petroleum potential of the San Joaquin basin, California, *in* Cram, I.H., ed., Future Petroleum Provinces of the United States—Their Geology and Potential: American Association of Petroleum Geologists, Memoir 15, p. 239–253.

Callaway, D.C., 1990, Organization of stratigraphic nomenclature for the San Joaquin basin, California, *in* Structure, Stratigraphy and Hydrocarbon Occurrences of the San Joaquin Basin, California: SEPM and American Association of Petroleum Geologists, Bakersfield, California, p. 5–22.

Carballo, J.D., Land, L.S., and Miser, D.E., 1987, Holocene dolomitization of supratidal sediments by active tidal pumping, Sugarloaf Key, Florida: Journal of Sedimentary Petrology, v. 57, p. 153–165.

Carothers, W.W., and Kharaka, Y.K., 1978, Alipathic acid anions in oil field waters implications for origin of natural gas: American Association of Petroleum Geologists, Bulletin, v. 62, p. 2441–2453.

Clayton, R.N., Freidman, I., Graf, D.L., Mayeda, T.K., Meents, W.F., and Shimp, N.F., 1966, The Origin of saline formation waters, I: isotopic composition: Journal of Geophysical Research, v. 71, p. 3869–3882.

Coleman, M.L., Curtis, C.D., and Irwin, H., 1986, Burial rate: Key to source and reservoir potential: World Oil, March, p. 83–92.

Craft, B.C., and Hawkins, M., 1991, Applied Petroleum Reservoir Engineering, 2nd edition revised by R.E. Terry: Englewood Cliffs, New Jersey, Prentice Hall, 431 p.

de Chambost E., Hillion F., Rasser B., and Migeon H.N., 1991, The CAMECA ims 1270: A description of the secondary ion optical system, *in* Benninghoven, H., ed., SIMS VIII Proceedings: New York, John Wiley & Sons, p. 207–210.

Deer, W.A., Howie, R.A., and Zussman, J., 1985, An Introduction to the Rock-Forming Minerals: New York, John Wiley & Sons, p. 473.

Dickinson, W.R., 1974, Plate tectonics and sedimentation, *in* Tectonics and Sedimentation: SEPM, Special Publication 22, p. 1–27.

Eiler, J.M., Valley, J.W., and Graham, C.M., 1997, Standardization of SIMS analysis of O and C isotope ratios in carbonates from ALH-84001: 28th Lunar and Planetary Science Conference, 3 p.

Feldman, M.D., Kwon, S.T., Boles, J.R., and Tilton, G.R., 1993, Diagenetic mass transport in the southern San Joaquin basin, California: Implications from strontium isotopic composition of modern pore fluids: Chemical Geology, v. 110, p. 329–343.

Fischer, K.S. and Surdam R.C., 1988, Contrasting diagenetic styles in a shelf turbidite sandstone sequence: the Santa Margarita and Stevens sandstones, San Joaquin basin, California, U.S.A, *in* Graham, S.A. ed., Studies of the Geology of the San Joaquin Basin: SEPM, Pacific section 60, p. 233–247.

Fisher, J.B., and Boles, J.R., 1990, Water–rock interaction in Tertiary sandstones, San Joaquin basin, California, U.S.A.: Diagenetic controls on water composition: Chemical Geology, v. 82, p. 83–101.

Friedman, I., and O'Neil, J.R., 1977, Compilation of stable isotope fractionation factors of geochemical interest, *in* Fleischer, M., ed., Data of Geochemistry, Chapter KK: U.S. Geological Survey, Professional Paper 440-KK, 60 p.

Fritz, P., and Smith, D.G.W., 1970, The isotopic composition of secondary dolomite: Geochimica et Cosmochimica Acta, v. 34, p. 1161–1173.

Giambalvo, E.R., Stein, S.R., and Fisher, A.T., 1997, Influence of bottom water temperature fluctuations on shallow thermal profiles in the Mariana Forearc: EOS, v. 78, No. 46, p. 717–718.

Graham, S.A., 1987, Tectonic controls on the petroleum occurrence in central California, *in* Ingersoll, R.V., and Ernst, W.G., eds., Cenozoic Basin Development of Coastal California; Ruby, Volume VI: Englewood Cliffs, New Jersey, Prentice Hall, p. 47–63.

Graham, S.A., and Williams, L.A., 1985, Tectonic, depositional, and diagenetic history of Monterey Formation, central San Joaquin basin, California: American Association of Petroleum Geologists, Bulletin 69, p. 385–411.

Hayes, J.B., 1979, Sandstone diagenesis—the whole truth, *in* Scholle, P.A., and Schluger, P.R., eds., Aspects of diagenesis: SEPM, Special Publication 26, p. 127–139.

Hayes, J.B., and Boles, J.R., 1992, Volumetric relations between dissolved plagioclase and kaolinite in sandstones: implications for mass transfer in the San Joaquin basin, California, *in* Houseknecht, D.W., and Pittman, E.D., Origin, Diagenesis, and Petrophysics of Clay Minerals in Sandstones: SEPM, Special Publication 47, p. 111–123.

Heald, M.T., and Larese, R.E., 1973, The significance of the solution of feldspar in porosity development: Journal of Sedimentary Petrology, v. 43, p. 458–460.

Hitchon, B., and Friedman, I., 1969, Geochemistry and origin of formation waters in the western Canada sedimentary basin, I: Stable isotopes of hydrogen and oxygen: Geochimica et Cosmochimica Acta, v. 33, p. 1321–1349.

Houseknecht, D.W., 1987, Assessing the relative importance of compaction processes and cementation to reduction of porosity in sandstones: American Association of Petroleum Geologists, Bulletin, v. 71, p. 633–642.

Hunt, J.M., 1979, Petroleum Geochemistry and Geology: San Francisco, W.H. Freeman & Co., 617 p.

James, A.T., and Baker, D.R., 1976, Oxygen isotope exchange between illite and water at 22°C: Geochimica et Cosmochimica Acta, v. 40, p. 235–239.

James, N.P., Bone Y., and Kyser T.K., 1993, Shallow burial dolomitization and dedolomitization of mid-Cenozoic cool water, calcitic, deep shelf limestone, southern Australia: Journal of Sedimentary Petrology, v. 63, p. 528–538.

Kyser, T.K., 1987, Equilibrium fractionation factors for stable isotopes, *in* Kyser, T.K., ed., Stable Isotope Geochemistry of Low Temperature Fluids: Mineralogical Association of Canada, Short Course 13, p. 1–84.

Lagoie, M.B., 1987, The stratigraphic record of sea level and climatic fluctuations in an active margin basin: The Stevens sandstones, North Coles Levee area, California: Palaios, v. 2, p. 48–68.

Leshin, L.A., McKeegan, K.D., Carpenter, P.K., and Harvey, R.P., 1998, Oxygen isotopic constraints on the genesis of carbonates from Martian meteorite ALH84001: Geochimica et Cosmochimica Acta, v. 62, p. 3–13.

Longstaffe, F.J., 1987, Stable isotopic studies of diagenetic processes, *in* Kyser, T.K., ed., Stable Isotope Geochemistry of Low Temperature Fluids: Mineralogical Association of Canada, Short Course 13, p. 187–257.

Longstaffe, F.J., Tilley, B.J., Ayalon, A., and Connolly, C.A., 1992, Controls on porewater evolution during sandstone diagenesis, Western Canada sedimentary basin: An oxygen iso-

tope perspective, in Origin, Diagenesis, and Petrophysics of Clay Minerals in Sandstones, SEPM, Special Publication 47, p. 13–34.

LONGSTAFFE, F.J., 1994, Stable isotopic constraints on sandstone diagenesis in the Western Canada sedimentary basin, *in* Parker, A., and Sellwood, B.W., eds., Quantitative diagenesis: Recent Developments and Applications to Reservoir Geology: Netherlands, Kulwar Academic Publishers, 223–274.

LUNDEGARD, P.D., 1985, Carbon dioxide and organic acids: origin and role in burial diagenesis (Texas Gulf Coast Tertiary), [unpublished Ph.D. dissertation]: University of Texas, Austin, Texas, 180 p.

MACGOWEN, D.B., AND SURDAM, R.C., 1988, Difunctional carboxylic acid anions in oil field water: Organic Geochemistry, v. 12, p. 245–259.

MAHON, K.I., HARRISON, T.M., AND GROVE, M., 1998a, The thermal and cementation histories of a sandstone petroleum reservoir, Elk Hills, California. Part 1: $^{40}Ar/^{39}Ar$ thermal results: Chemical Geology, v. 152, p. 227–256.

MAHON, K.I., HARRISON, T.M., AND MCKEEGAN, K.D., 1998b, The thermal and cementation histories of a sandstone petroleum reservoir, Elk Hills, California. Part 2: *In situ* oxygen and carbon isotopic results: Chemical Geology, v. 152, p. 257–271.

MAZZULLO, S.J., BISCHOFF, W.D., AND TEAL, C.S., 1995, Holocene shallow-subtidal dolomitization by near-normal seawater, Northern Belize: Geology, v. 23, p. 341–344.

MOZLEY, P.S., 1989, Relation between depositional environment and the elemental composition of early diagenetic siderite: Geology, v. 17, p. 704–706.

O'NEIL, J.R. AND KHARAKA, Y.F., 1976, Hydrogen and oxygen isotope exchange reactions between clay minerals and water: Geochimica et Cosmochimica Acta, v. 40, p. 241–246.

PATE, C.R., 1989, Assessing the relative importance of compaction processes and cementation to reduction of porosity in sandstones: Discussion: American Association Petroleum Geologists, Bulletin, v. 73, p. 1270–1273.

PETERS, K.E., ELAM, T.D., PYTTE, M.H., AND SUNDARARAMAN, P., 1994, Identification of petroleum systems adjacent to the San Andreas Fault, California, U.S.A., *in* Magoon, L.B., and Dow, W.G., eds., The Petroleum System—From Source to Trap: American Association of Petroleum Geologists, Memoirs 60, p. 423–436.

REID, S.A., 1990, Trapping characteristics of upper Miocene turbidite deposits, Elk Hills field, Kerm County, California, *in* Structure, Stratigraphy, and Hydrocarbon Occurrences of the San Joaquin basin, California: SEPM and American Association of Petroleum Geologists, Bakersfield, California, p. 5–22.

RICIPUTI, L.R., PATERSON, B.A., AND RIPPERDAN, R.L., 1998, Measurement of light stable isotope ratios by SIMS: Matrix effects for oxygen, carbon, and sulfur isotopes in minerals: International Journal of Mass Spectrometry and Ion Processes, v. 178, p. 81–112.

ROBINSON, A.G., COLEMAN, M.L., AND GLUYAS, J.G., 1993, The age of illite cement growth, Village Fields area, southern North Sea: evidence from K-Ar ages and $^{18}O/^{16}O$ ratios: American Association of Petroleum Geologists, Bulletin, v. 77, p. 68–80.

SAVIN, S.M., 1977, The history of the Earth's temperature during the past 100 million years: Annual Review of Earth and Planetary Sciences, v. 5, p. 319–355.

SAVIN, S.M., 1980, Oxygen and hydrogen isotope effects in low-temperature mineral–water interactions, *in* Fritz, A.P., and Fontes, J. Ch., eds., The Terrestrial Environment: Handbook of Environmental Isotope Geochemistry, v. 1, Amsterdam, Elsevier, v. 1, p. 283–327.

SAVIN, S.M. AND YEH, H-W., 1981, Stable isotopes in ocean sediments, *in* Emiliani, C., ed., The Sea, v. 7, The Oceanic Lithosphere, New York, John Wiley & Sons, p. 1521–1554.

SCHULTZ, J.L., BOLES, J.R., AND TILTON, G.R., 1989, Tracking calcium in the San Joaquin basin, California: A strontium isotopic study of carbonate cements at North Coles Levee: Geochimica et Cosmochimica Acta, v. 53, p. 1991–1999.

SHARP, J.M., JR., GALLOWAY, W.E., LAND, L.S., MCBRIDE, E.F., BLANCHARD, P.E., BODNER, D.P., DUTTON, S.P., FARR, M.R., GOLD, P.B., JACKSON, T.J., LUNDEGARD, P.D., MACPHERSON, G.L., AND MILLIKEN, K.L., 1988, Diagenetic processes in north-western Gulf of Mexico sediments, *in* Chillingarian, G.V. and Wolf, K.H., eds., Diagenesis, II: Amsterdam, Elseveir, Developments in Sedimentology, v. 43, p. 43–113.

SLODZIAN, G., CHAINTEAU, M.P., AND DENNEBOUY, R.C., 1987, SIMS: Self-regulated potential at insulating surfaces in presence of strong electrostatic field: CAMECA News, May, 1987.

SUCHECKI, R.K., AND LAND, L.S., 1983, Isotope geochemistry of burial-metamorphosed volcanogenic sediments, Great Valley sequence, northern California: Geochimica et Cosmochimica Acta, v. 47, p. 1487–1499.

TAYLOR, T.R., AND SOULE, C.H., 1993, Reservoir characterization and diagenesis of the Oligocene 64-Zone sandstone, North Belridge field, Kern County, California: American Association of Petroleum Geologists, Bulletin, v. 77, p. 1549–1566.

VALLEY, J.W., GRAHAM, C.M., HART, B., EILER, J.M., AND KINNY, P.D., 1997, Ion microprobe analysis of oxygen, carbon, and hydrogen isotope ratios, *in* McKibben, M.A., and Shanks, W.C., eds., Applications of Microanalytical Techniques to Understanding Mineralizing Processes: Society of Economic Geologists, Reviews, v. 7, p. 73–98.

WOOD, J.R., AND BOLES, J.R., 1991, Evidence for episodic cementation and diagenesis recording of seismic pumping events, North Coles Levee, California, U.S.A: Applied Geochemistry, v. 6, p. 509–521.

WOODRUFF, R., SAVIN, S.M., AND DOUGLASS, R.E., 1981, Miocene stable isotope record: A detailed deep Pacific Ocean study and its paleoclimatic implications: Science, v. 212, p. 665–668.

Received 18 May 1999; accepted 11 July 2000.